

Electronic supporting information for

Luminescent pro-Nitroxide Lanthanide Complexes for the Detection of Reactive Oxygen Species

Richard Barré, Damien Mouchel dit Leguerrier, Lionel Fedele, Daniel Imbert, Jennifer K. Molloy,
Fabrice Thomas

Content

1. Experimental	S2
2. Figures	S5
3. Tables.....	S25
4. References.....	S26

1. Experimental

1.1 Materials and methods

All chemicals were of reagent grade and were used without purification. Lanthanide nitrate salts were purchased from Aldrich and titrated for metal content before use, in the presence of EDTA and xylene orange. High resolution mass spectra were recorded on a Waters Xevo G2-S QToF apparatus. NMR spectra were recorded on Bruker Avance III spectrometer (^1H at 400 MHz or 500 MHz). Chemical shifts are quoted relative to tetramethylsilane (TMS).

1.2 Synthetic procedures

2-(Chloromethyl)-6-(4,4,5,5-tetramethylimidazolidin-2-yl)pyridine (2)

A solution of 2,3-dimethylbutane-2,3-diamine hydrosulfate (0.300 g, 1.22 mmol) in H_2O (10 mL) was added to a solution of 6-(chloromethyl)pyridine-2-carbaldehyde (0.190 g, 1.22 mmol)¹ in methanol (10 mL) with vigorous stirring. Sodium acetate (120 mg, 1.46 mmol) was added to the reaction and the yellow solution turned turbid after 30 min and a white precipitate formed. The mixture was then stirred overnight at room temperature and the white solid was filtered and dried under vacuum to obtain the desired product (0.273 g, 78% yield). ^1H NMR (500 MHz, DMSO-d_6) δ / ppm 7.85 (t, $^3J_{\text{H-H}} = 8\text{Hz}$, 1H); 7.56 (d, $^3J_{\text{H-H}} = 8\text{Hz}$, 1H); 7.43 (d, $^3J_{\text{H-H}} = 8\text{Hz}$, 1H); 4.76 (s, 2H); 4.63 (s, 1H), 1.07 (d, $^3J_{\text{H-H}} = 4\text{Hz}$, 12H). ^{13}C NMR (125 MHz, DMSO-d_6) δ / ppm = 161.9 (Ar), 155.2 (Ar), 137.7 (Ar), 122.6 (Ar), 122.5 (Ar), 91.6 (imidazole), 66.9 (C-quat), 66.8 (C-quat), 47.5 (CH_2Cl), 24.5 (CH_3), 17.9 (CH_3). HR-MS (ESI) m/z calcd. for $\text{C}_{13}\text{H}_{21}\text{O}_2\text{N}_3\text{Cl}$ $[\text{M}+\text{H}]^+$ 286.1317, found 286.1127. IR (cm^{-1}): 3245, 2984, 1594, 1448, 1377, 1045, 995, 719, 580.

2-(chloromethyl)-6-(1-hydroxy-4,4,5,5-tetramethyl-imidazol-2-yl)pyridine (3)

Sodium periodate (0.019 g, 0.089 mmol) was added to solution of (2) (0.017 g, 0.059 mmol) in a mixture of dichloromethane (5 mL), ethyl acetate (2.5 mL) and water (5 mL). After 5 minutes, the solution turned deep purple. The reaction mixture was stirred during 30 minutes at room temperature while the reaction was monitored by TLC using silica plates. The aqueous phase was extracted with dichloromethane (10 mL), the organic phases were combined, dried with Na_2SO_4 and the solvent was removed *in vacuo* to afford the product (3) as a purple powder (0.016 g, 88%). HR-MS (ESI) m/z calcd for $\text{C}_{13}\text{H}_{18}\text{O}_2\text{N}_3\text{Cl}$ $[\text{M}+\text{H}]^+$ 283.1082, found 283.1081. IR (cm^{-1}): 2965, 2918, 2851, 1359, 1087, 705, 643.

$^t\text{Bu}_3\text{L}$ (4)

$\text{DO}_3\text{A}^t\text{Bu}$ (0.071 g, 0.138 mmol) was dissolved in anhydrous acetonitrile (25 mL) and potassium carbonate (0.038 g, 0.276 mmol) was added. After 5 minutes of stirring, (3) (0.038 g, 0.138 mmol) and potassium iodide (0.023 g, 0.138 mmol) were added and the reaction was stirred under argon for 48 h. The suspension was filtered on a sintered glass funnel and the filtrate was diluted with water (5 mL). The solution was extracted with dichloromethane (3 x 15 mL), organic phases were combined, dried with Na_2SO_4 and the solvent was removed under vacuum to afford the desired product (4) as a purple solid (0.101 g, 97% yield). HR-MS (ESI) m/z calcd for $\text{C}_{39}\text{H}_{67}\text{O}_8\text{N}_7$ $[\text{M}+\text{H}]^+$ 761.5046, found 761.5045. IR (cm^{-1}): 2975, 2930, 2850, 1724, 1367, 1153, 1101.

Ligand H₃L (5)

^tBu₃L (4) (0.101 g, 0.133 mmol) was dissolved in dichloromethane (14 mL) and anhydrous trifluoroacetic acid (2 mL) was added to the reaction. The reaction instantly underwent a colour change from intense purple to pale yellow upon the addition. The solution was stirred overnight and trifluoroacetic acid was removed under vacuum. The oil was redissolved in dichloromethane and evaporated again three times and the same procedure was done with methanol to eliminate all traces of trifluoroacetic acid. Then the oily residue was redissolved in a minimum of methanol and upon addition of diethyl ether, a yellow precipitate was observed. The solid was recovered and triturated with diethyl ether and the excess of solvent was removed by decantation. The solid was dried *in vacuo* to obtain the crude product. Purification by exclusion chromatography LH-20 Sephadex in water afforded the pure product H₃L (5) as a yellow powder (0.067 g, 83%). ¹H NMR (500 MHz, D₂O) δ/ ppm 8.22 (d, ³J_{H-H} = 8Hz, 1H), 8.13 (d, ³J_{H-H} = 8Hz, 1H), 8.04 (t, ³J_{H-H} = 8Hz, 1H), 3.53-3.30 (br, 15H) 3.25-2.89 (br, 16H), 1.46 (d, ³J_{H-H} = 6Hz, 12H). ¹³C NMR (125 MHz, D₂O) δ/ ppm 174.4, 169.8, 163.3, 163.1, 162.8, 162.5, 159.9, 140.2, 139.5, 130.1, 125.8, 117.5, 115.2 112.8, 74.4, 66.0, 63.9, 58.2, 57.4, 56.2, 55.8, 53.4, 53.2, 51.6, 51.3, 50.4, 49.0, 48.0, 47.8, 42.3, 21.7, 18.0, 16.8. HR-MS (ESI) m/z calcd for C₂₇H₄₄O₇N₇ [M+H]⁺ 578.3297, found 578.3275. IR (cm⁻¹): 2990, 1673, 1399, 1173, 1124, 799, 719.

1.3 EPR spectra

X-band EPR spectra were recorded on a Bruker EMX Plus spectrometer controlled with the Xenon software and equipped with a high sensitivity resonator. The spectra were simulated by using the Easyspin² software. The intensities are calculated from the heights of the lines at 334.4 mT (low field resonance of the nitronylnitroxide radical – no signal for the iminonitroxide radical) and 335.0 mT (low field resonance of the iminonitroxide radical – no signal for the nitronylnitroxide radical). The maximum intensity is set at 100 % and the intensities at given times are expressed in ratio of this maximum signal intensity and fitted with the OriginLab Origin Pro 8 software (Table S1).

1.4 Luminescence spectra

Luminescence spectra of the lanthanide complexes were recorded using a modular Fluorolog FL3-22 spectrometer Horiba-Jobin Yvon-Spex equipped with a double grating excitation monochromator and an iHR320 imaging spectrometer. Hamamatsu R928P and Hamamatsu R5509 photomultipliers were used for visible and NIR measurements, respectively. All spectra were corrected for detection and optical spectral response (instrumental functions) of the spectrofluorimeters. Quartz capillaries of 4 mm in diameter were used. For the acquisition of the excitation and emission spectra in the NIR, a long pass coloured filter was used at 870 nm to block the signal of the 2nd harmonics. Phosphorescence lifetimes of the lanthanides were measured in time-resolved mode and are the averages of three independent measurements that were taken by monitoring the decay at the maxima of the emission spectra. The signals were analyzed with the OriginLab Origin Pro software. Lifetimes of singlet states were obtained using nanoled sources S-390 (FWHM 15 nm) from Horiba Scientific coupled to a Jobin Yvon NL-C2 Pulse Diode controller and a DH-HT TCSPC controller including a

SpectraLED output. The output signal of the photomultiplier was fed to a PC and controlled and analyzed with the Data Station (v2.7) and Decay Analysis (v6.8) software from Horiba Scientific. Lifetimes are averages of 3 independent determinations with a calculated Chi-square < 2.

1.5 Electrochemistry

Cyclic voltammetry curves were recorded using a CHI 620 potentiostat. The measurements were performed in 0.5 mM CH₃CN solutions containing 0.1 M tetra-*n*-butyl ammonium perchlorate (TBAP) as supporting electrolyte. In the case of **5**, **5Eu** and **5Yb** 2 % of water was added to improve the solubility. Experiments were performed in a standard three-electrode cell under argon atmosphere. A glassy carbon disc electrode (3 mm diameter), which was polished with 1 mm diamond paste, was used as the working electrode. The auxiliary electrode is a compartmentalized platinum wire, while an Ag/AgNO₃ 0.01 M electrode was used as reference.

2. Figures

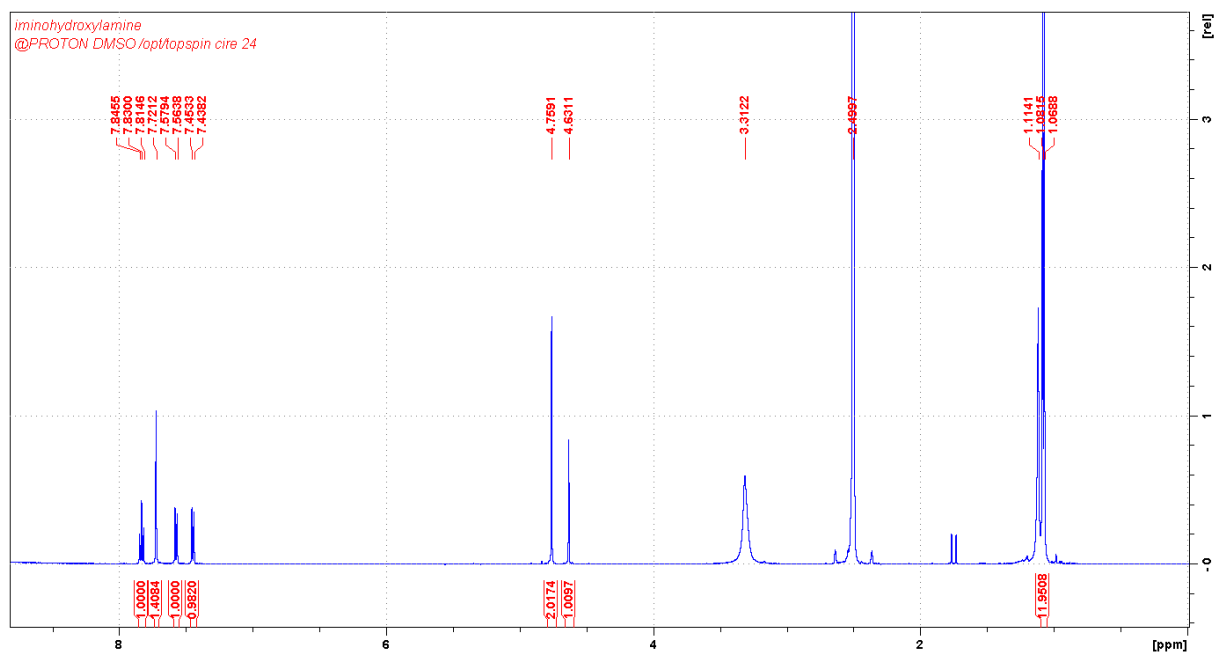


Fig S1. ^1H NMR spectrum of **2** (500 MHz, $\text{DMSO-}d_6$, 298K)

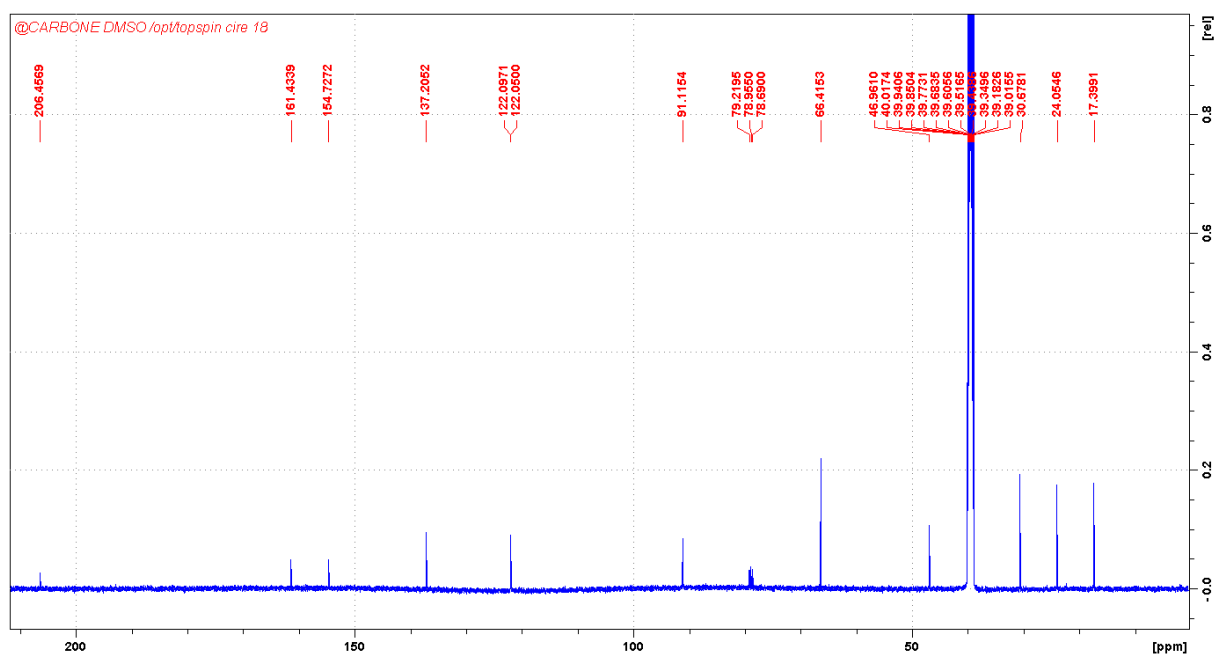


Fig S2. ^{13}C NMR spectrum of **2** (500 MHz, $\text{DMSO-}d_6$, 298K)

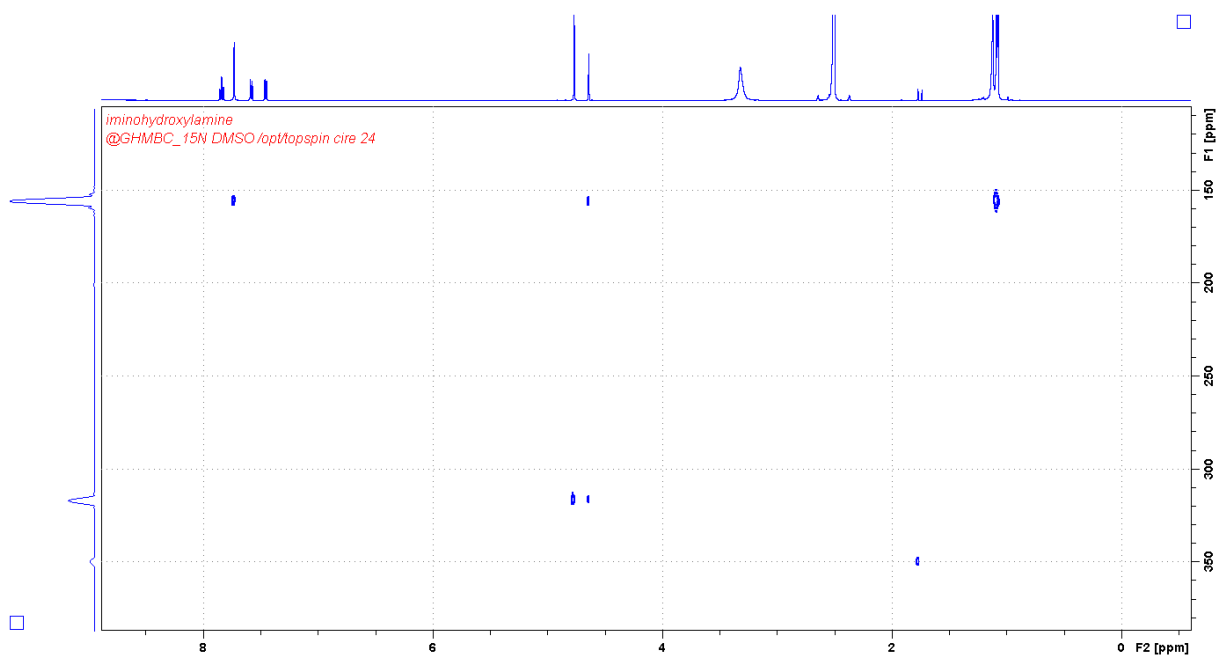


Fig S3. ^1H - ^{15}N HMBC spectrum of **2** (500 MHz, $\text{DMSO-}d_6$, 298K)

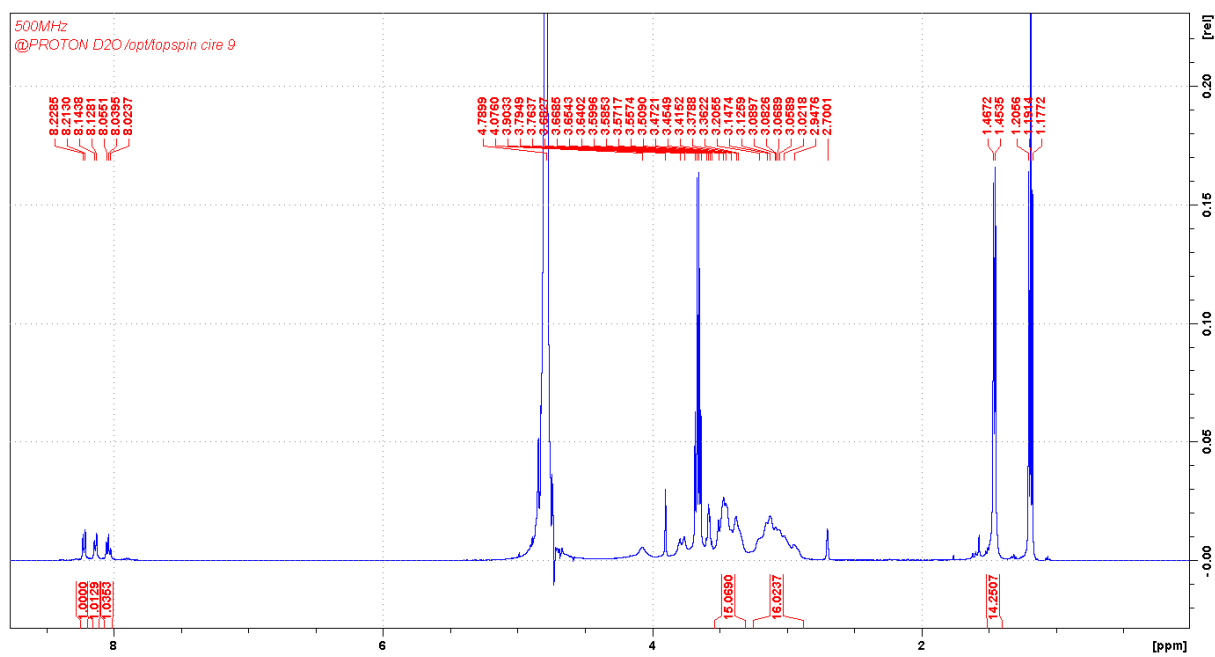


Fig S4. ^1H NMR spectrum of **5** (500 MHz, D_2O , 298K)

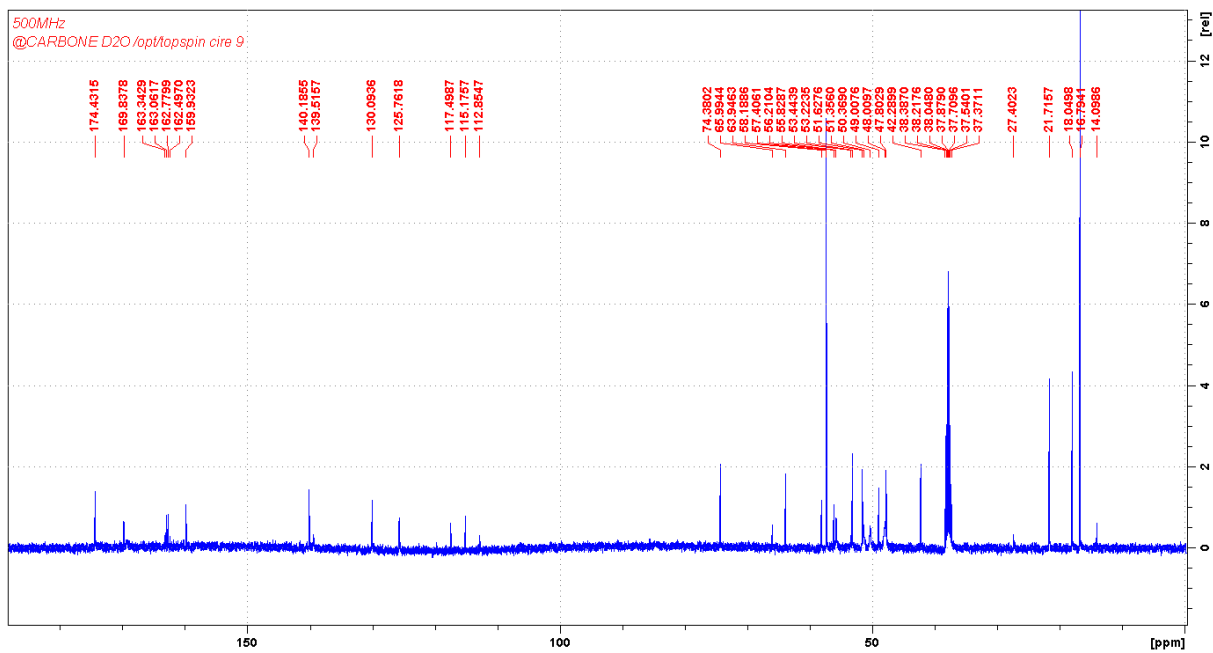


Fig S5. ^{13}C NMR spectrum of **5** (500 MHz, D_2O , 298K)

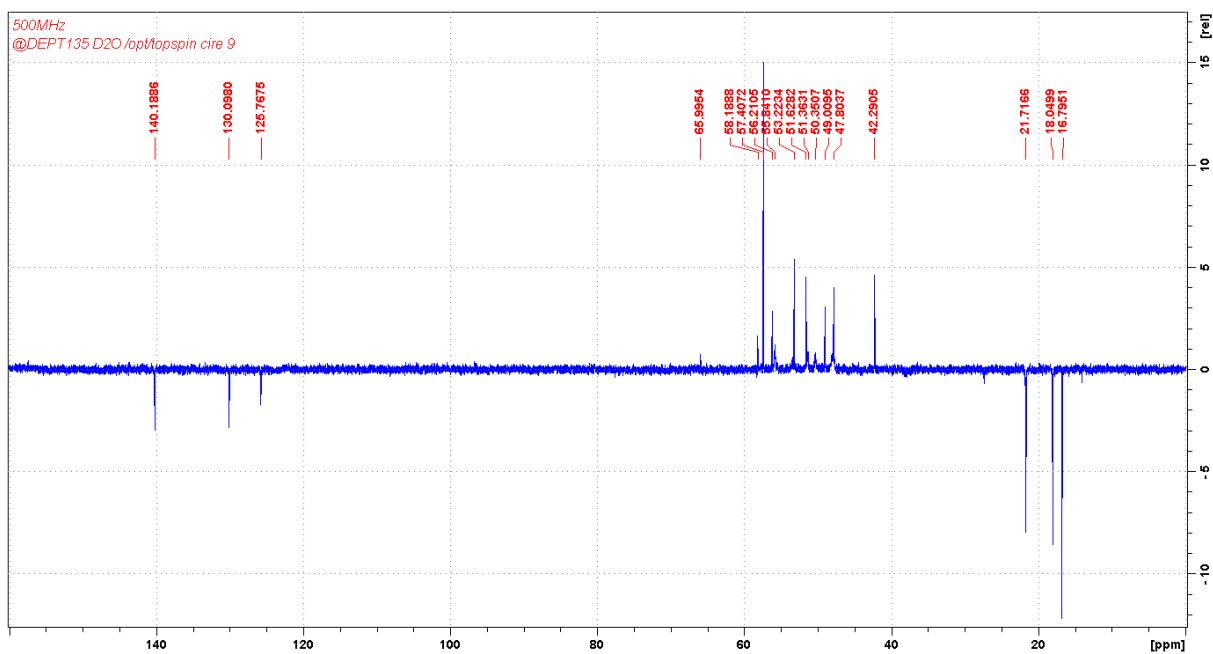


Fig S6. ^{13}C NMR spectrum of **5** (DEPT 135, 500 MHz, D_2O , 298K)

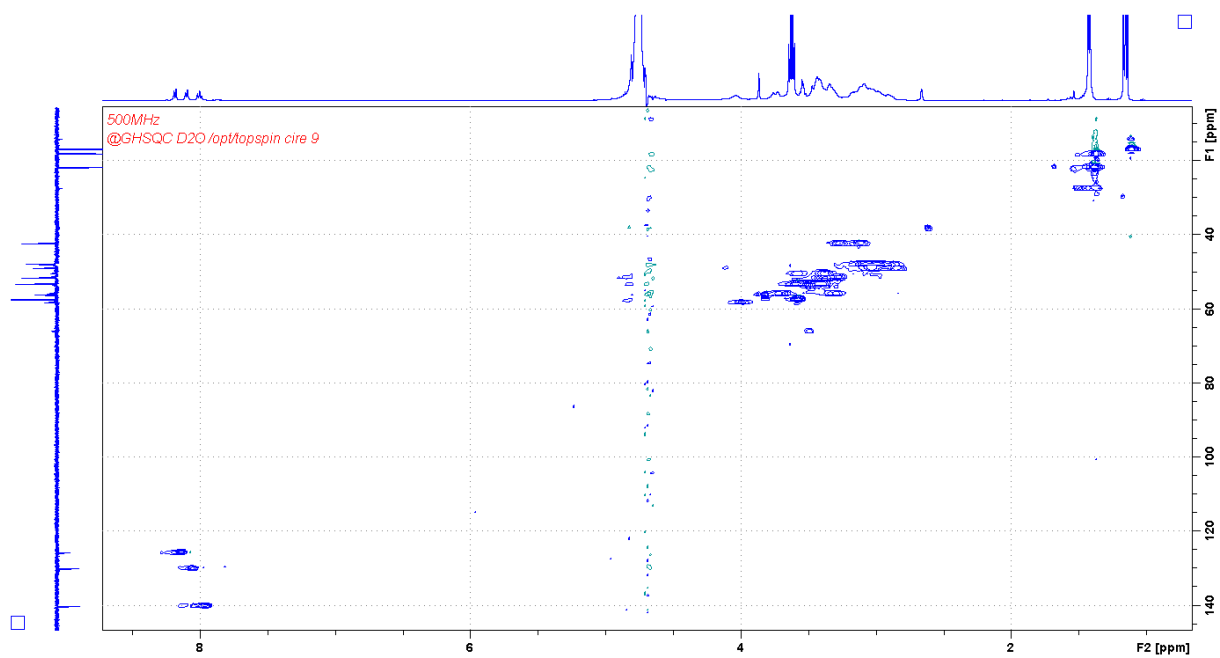


Fig S7. ^1H - ^{13}C HSQC NMR spectrum of **5** (500 MHz, D_2O , 298K)

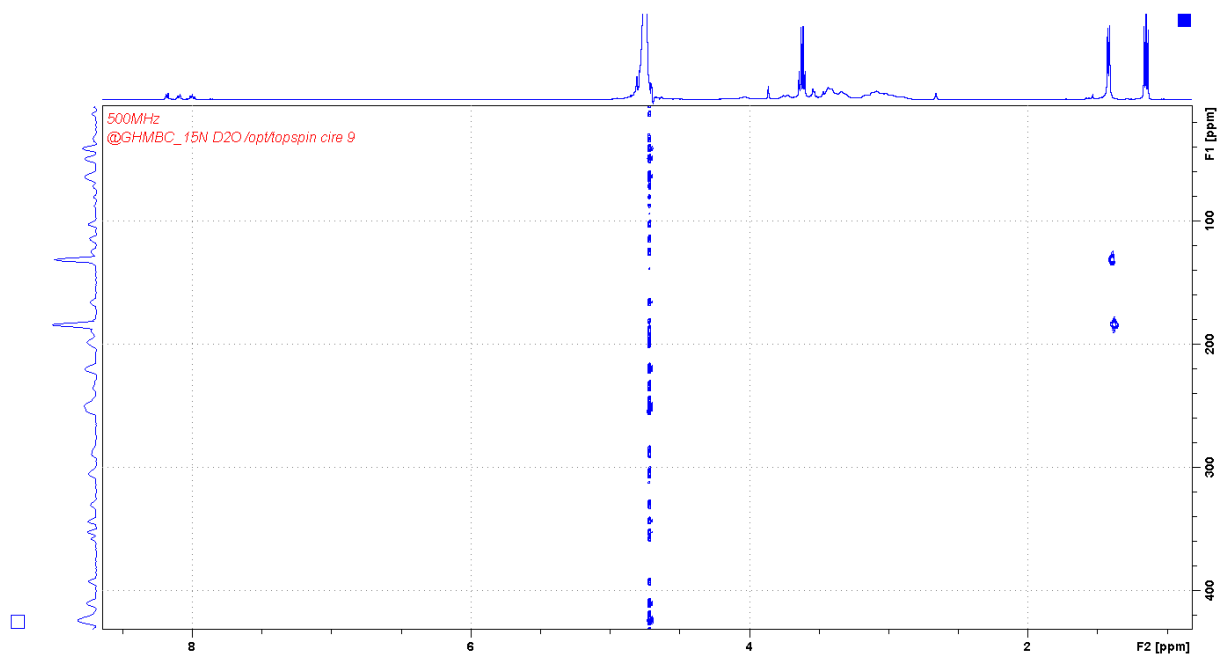


Fig S8. ^1H - ^{15}N HMBC NMR spectrum of **5** (500 MHz, D_2O , 298K)

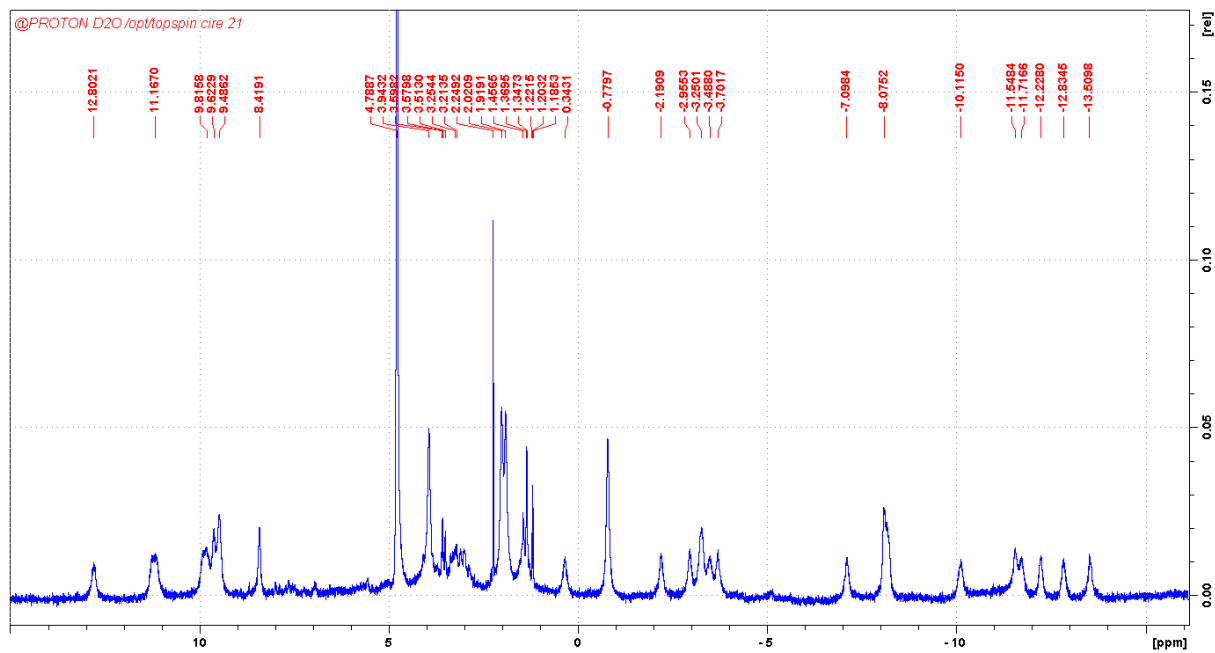


Fig S9. ^1H NMR spectrum of **5Eu** (400 MHz, D_2O , 298K)

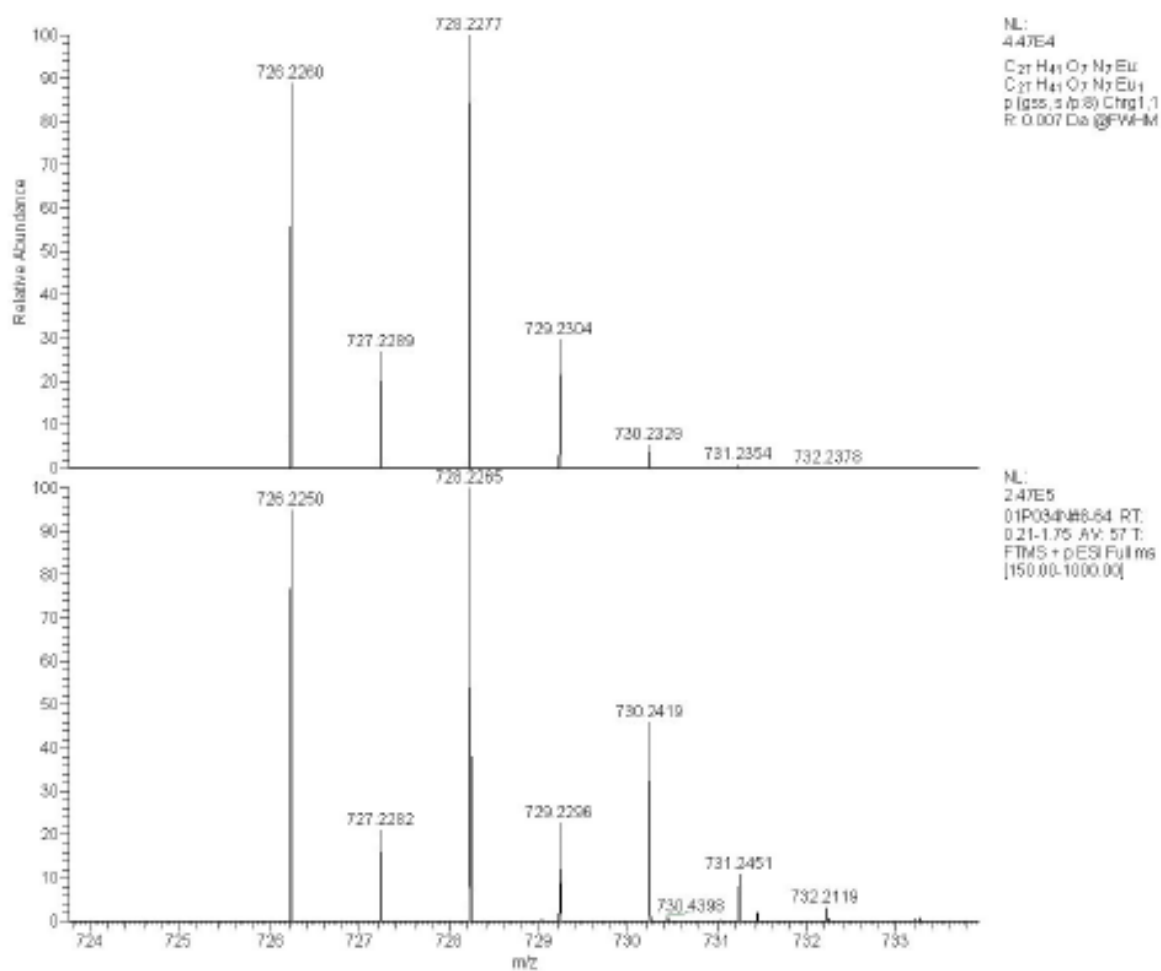


Fig S10. HRMS of **5Eu**: (top) calculated, (bottom) experimental. The expected peak for C₂₇H₄₁N₇O₇Eu ([M+H]⁺) is 728.227991.

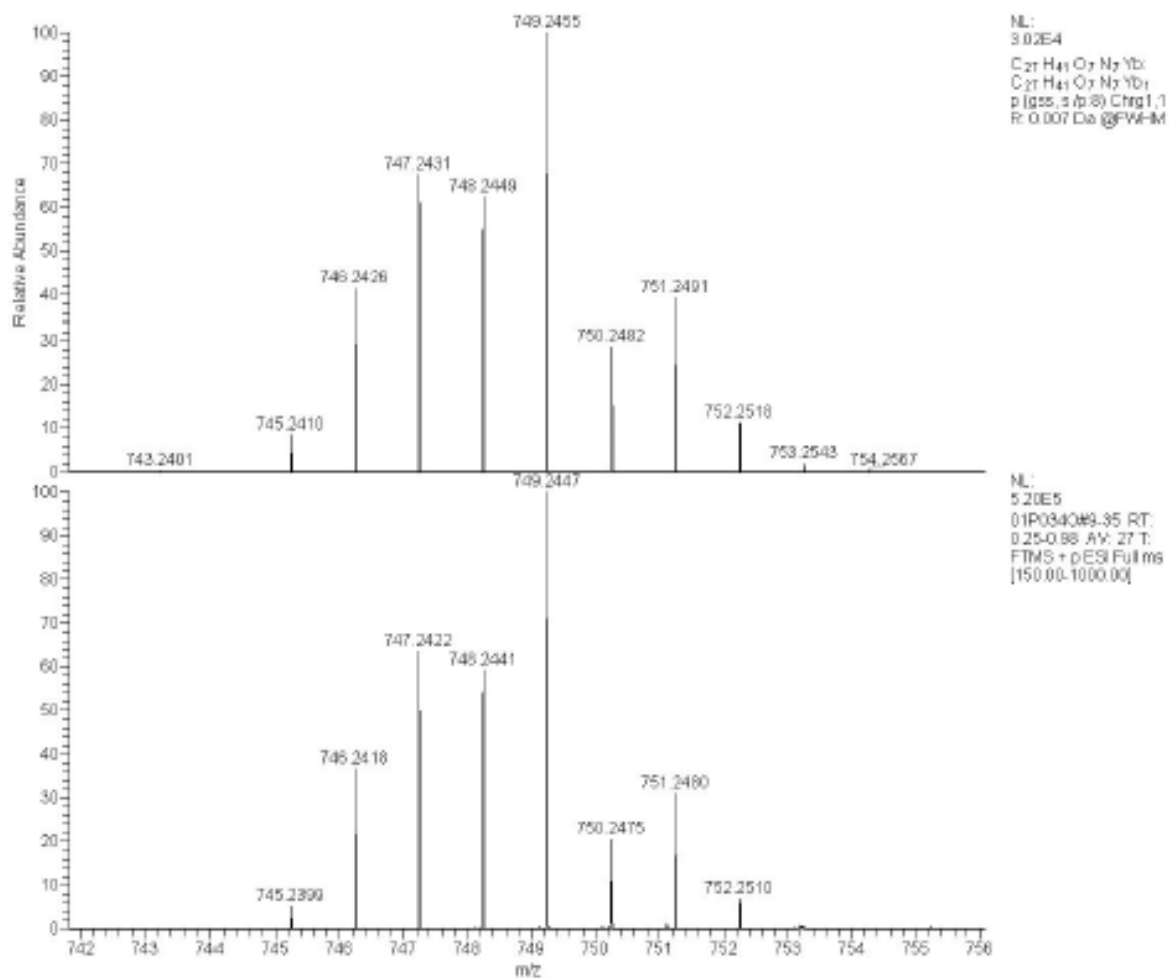


Fig S11. HRMS of **5Yb**: (top) calculated, (bottom) experimental. The expected peak for C₂₇H₄₁N₇O₇Yb ([M+H]⁺) is 749.245621.

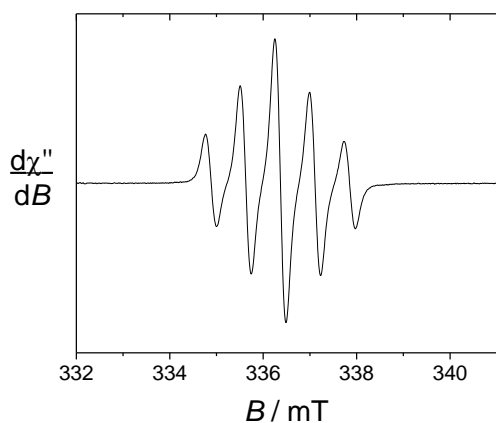


Fig S12. Isotropic EPR spectrum of **3** (3.5 mM) in DMF. Microwave Freq. 9.44 GHz, power 1.8 mW; Mod. Amp. 0.2 mT, Freq. 100 KHz; $T = 293$ K.

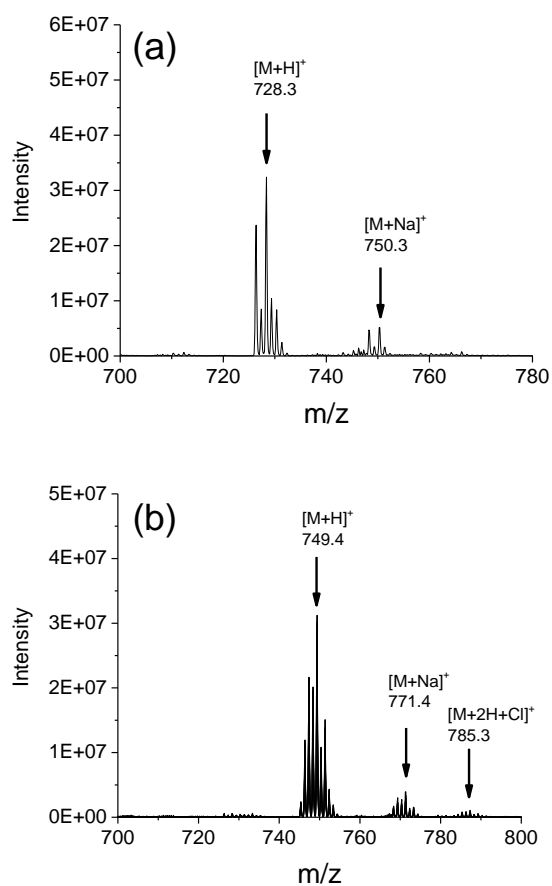


Fig S13. ESI-MS in positive mode of (a) **5Eu** and (b) **5Yb**. The aqueous solutions are diluted to 10^6 in CH_3CN before injection. The exact mass for **5Eu** ($\text{C}_{27}\text{H}_{40}\text{N}_7\text{O}_7\text{Eu}$) and **5Yb** ($\text{C}_{27}\text{H}_{40}\text{N}_7\text{O}_7\text{Yb}$) are 727.227991 and 748.245621, respectively.

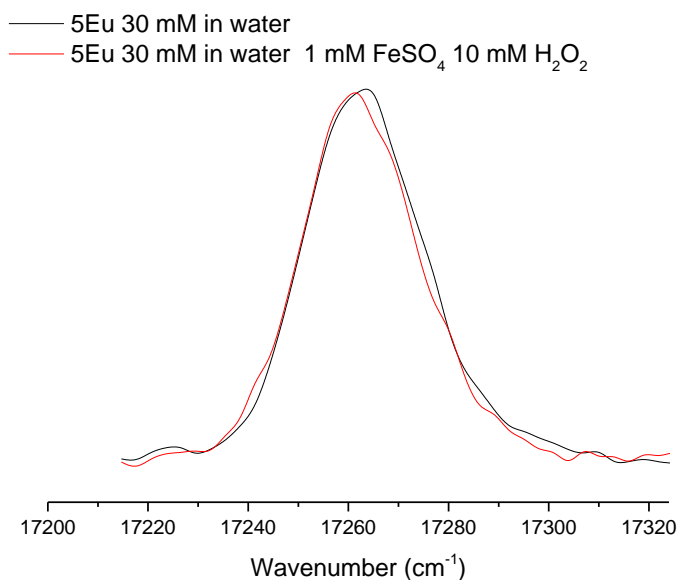


Fig S14. Normalized emission spectra ($\lambda_{\text{ex}} = 325 \text{ nm}$) of the $^5\text{D}_0 \rightarrow ^7\text{F}_0$ transition of **5Yb** in 0.03 M aqueous solutions after 6 days. Dark blue = Blank; Black line = after 6 days in reaction with 10 mM H₂O₂ and 1 mM FeSO₄. $T = 293 \text{ K}$.

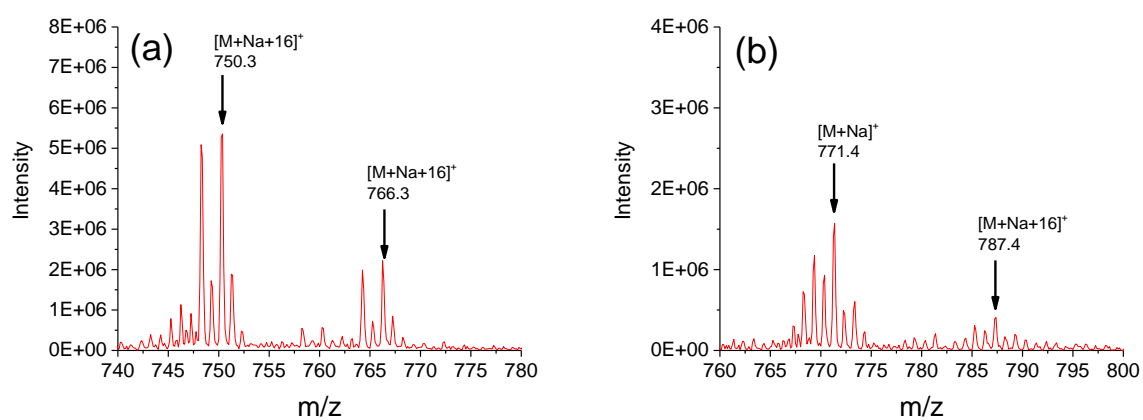


Fig S15. Zoom of the ESI-MS in positive mode of (a) **5Eu** and (b) **5Yb** (0.03 M) after reaction with 10 mM H₂O₂ and 1 mM FeSO₄ in H₂O (6 days). The solutions are diluted to 10⁶ in CH₃CN before injection.

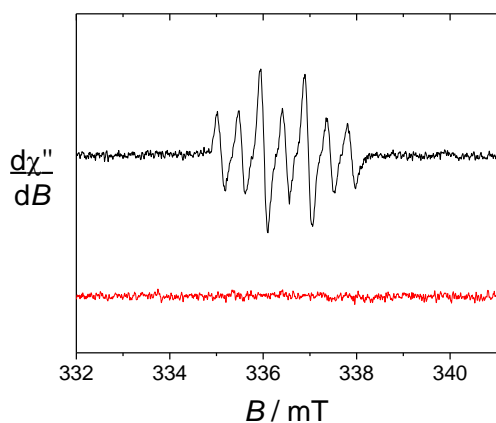


Fig S16. Isotropic EPR spectra of **5Eu** (0.03 M) in (red) H₂O and (black) upon reaction with 10 mM H₂O₂ and 1 mM FeSO₄ in H₂O (3 min). Microwave Freq. 9.44 GHz, power 1.8 mW; Mod. Amp. 0.2 mT, Freq. 100 KHz; *T* = 293 K.

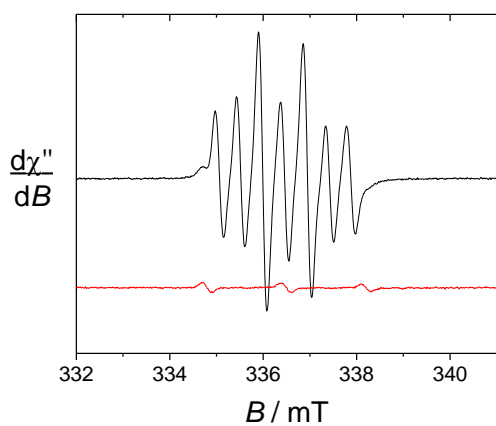


Fig S17. Isotropic EPR spectra of **5Yb** (0.03 M) in (red) H₂O and (black) upon reaction with 10 mM H₂O₂ and 1 mM FeSO₄ in H₂O (3 min). Microwave Freq. 9.44 GHz, power 1.8 mW; Mod. Amp. 0.2 mT, Freq. 100 KHz; *T* = 293 K.

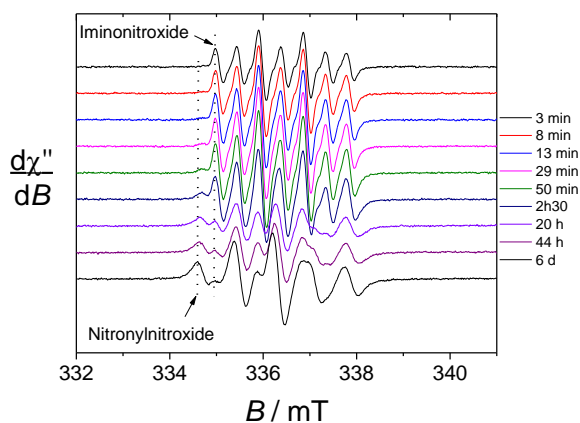


Fig S18. Isotropic EPR spectra of **5Eu** (0.03 M) upon reaction with 10 mM H_2O_2 and 1 mM FeSO_4 in H_2O . Microwave Freq. 9.44 GHz, power 1.8 mW; Mod. Amp. 0.2 mT, Freq. 100 KHz; $T = 293$ K.

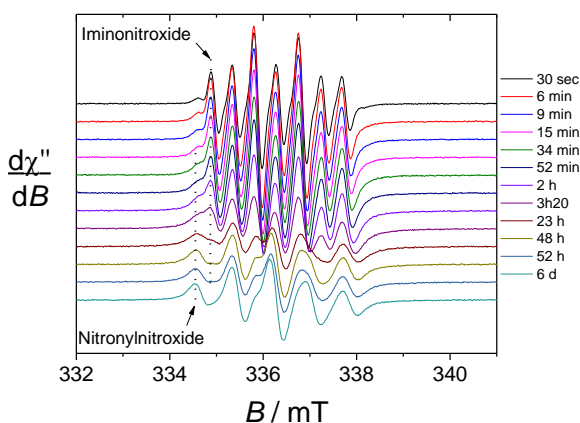


Fig S19. Isotropic EPR spectra of **5Yb** (0.03 M) upon reaction with 10 mM H_2O_2 and 1 mM FeSO_4 in H_2O . Microwave Freq. 9.44 GHz, power 1.8 mW; Mod. Amp. 0.2 mT, Freq. 100 KHz; $T = 293$ K.

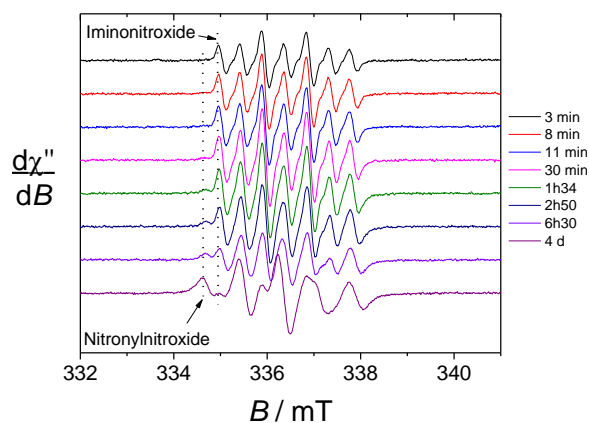


Fig S20. Isotropic EPR spectra of 5Eu (0.03 M) upon reaction with $10\text{ mM H}_2\text{O}_2$ and 1 mM FeSO_4 in buffered (Tris/HCl 0.05 M) H_2O solution at pH 7. Microwave Freq. 9.44 GHz, power 1.8 mW; Mod. Amp. 0.2 mT, Freq. 100 KHz; $T = 293\text{ K}$.

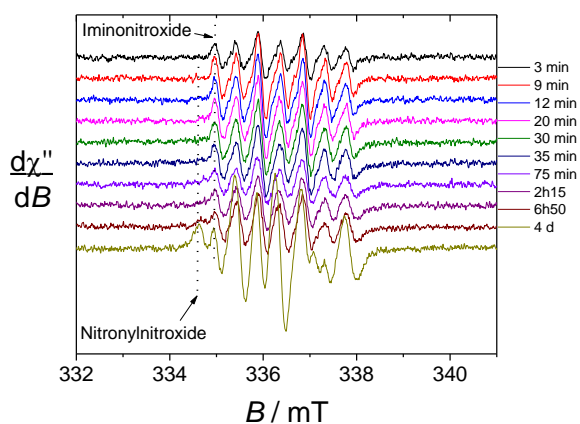


Fig S21. Isotropic EPR spectra of 5Yb (0.03 M) upon reaction with $10\text{ mM H}_2\text{O}_2$ and 1 mM FeSO_4 in buffered (Tris/HCl 0.05 M) H_2O solution at pH 7. Microwave Freq. 9.44 GHz, power 1.8 mW; Mod. Amp. 0.2 mT, Freq. 100 KHz; $T = 293\text{ K}$.

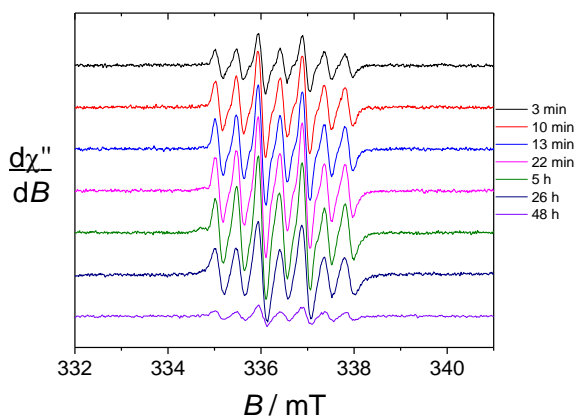


Fig S22. Isotropic EPR spectra of 5Eu (0.03 M) upon reaction with 10 mM H_2O_2 and 1 mM FeSO_4 in H_2O containing DMSO. Microwave Freq. 9.44 GHz, power 1.8 mW; Mod. Amp. 0.2 mT, Freq. 100 KHz; $T = 293$ K.

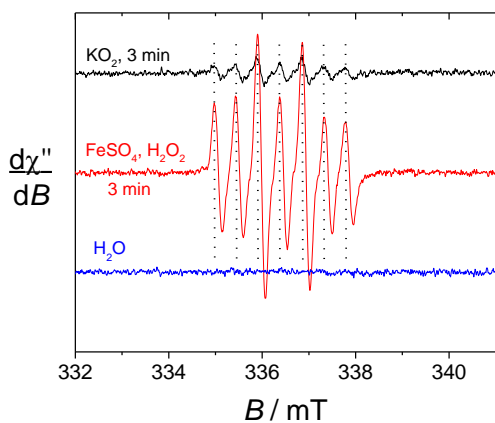


Fig S23. Isotropic EPR spectra of 5Eu (0.03 M) upon reaction with (black) KO_2 (saturated solution) in H_2O (3 min); (red) 10 mM H_2O_2 and 1 mM FeSO_4 in H_2O (3 min); (blue) blank in H_2O . Microwave Freq. 9.44 GHz, power 1.8 mW; Mod. Amp. 0.2 mT, Freq. 100 KHz; $T = 293$ K.

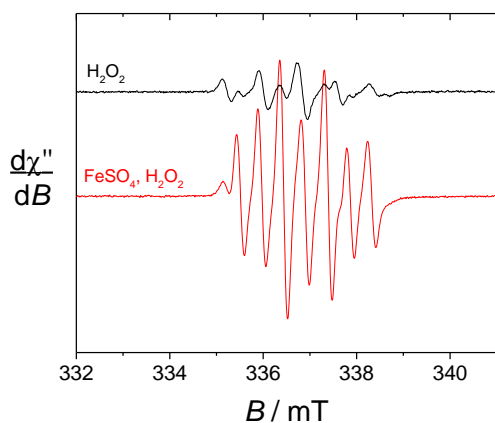


Fig S24. Isotropic EPR spectra of **5Eu** (0.03 M) upon reaction with (black) 10 mM H_2O_2 and (red) 10 mM H_2O_2 and 1 mM FeSO_4 in H_2O (40 min). Microwave Freq. 9.44 GHz, power 1.8 mW; Mod. Amp. 0.2 mT, Freq. 100 KHz; $T = 293$ K.

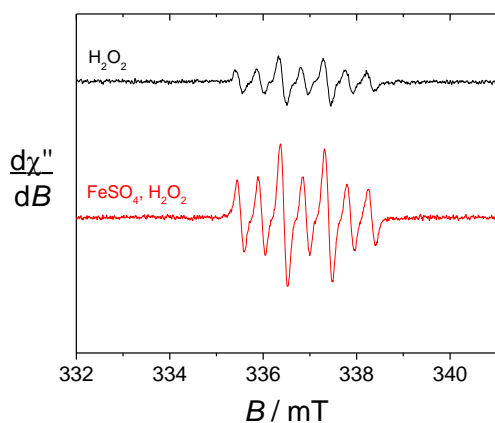


Fig S25. Isotropic EPR spectra of **5Yb** (0.03 M) upon reaction with (black) 10 mM H_2O_2 and (red) 10 mM H_2O_2 and 1 mM FeSO_4 in H_2O (10 min). Microwave Freq. 9.44 GHz, power 1.8 mW; Mod. Amp. 0.2 mT, Freq. 100 KHz; $T = 293$ K.

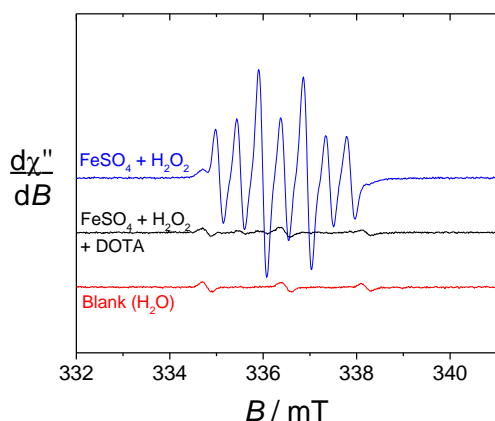


Fig S26. Isotropic EPR spectra of **5Yb** (0.03 M) upon reaction with (blue) 10 mM H_2O_2 and 1 mM FeSO_4 in H_2O (3 min); (black) 1.2 equiv. DOTA + 10 mM H_2O_2 and 1 mM FeSO_4 in H_2O (3 min); (red) blank in H_2O . Microwave Freq. 9.44 GHz, power 1.8 mW; Mod. Amp. 0.2 mT, Freq. 100 KHz; $T = 293$ K.

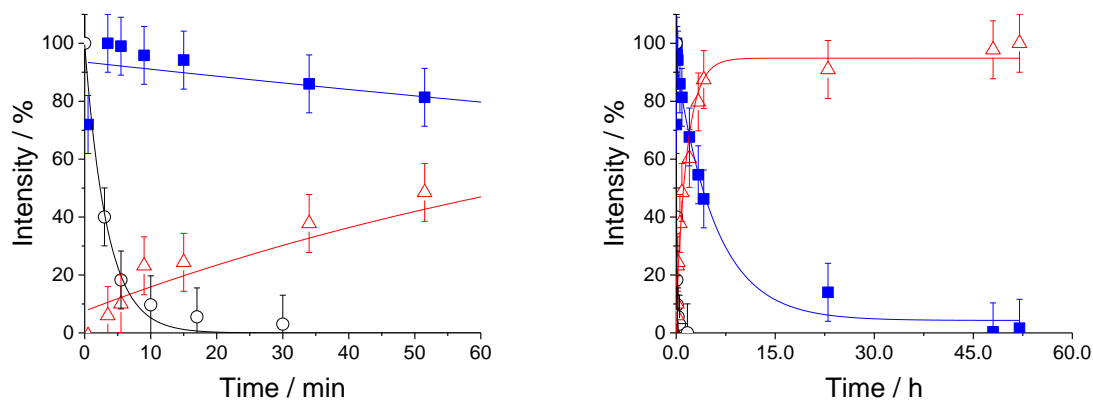


Fig S27. Evolution of the maximum intensity of the EPR signal as a function of time for a 0.03 M solution of **5Yb** (solid blue squares: iminonitroxide radical; open red triangles: nitronyl nitroxide radical) and 0.05 M solution of DMPO (0.05 M, open black circles) in the presence of 10 mM H_2O_2 and 1 mM FeSO_4 in H_2O at $T = 293$ K.

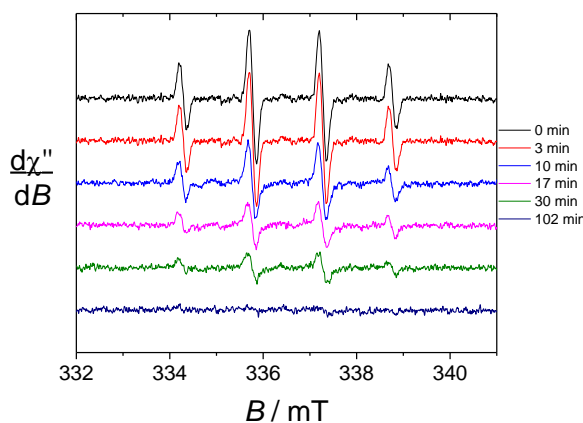


Fig S28. Isotropic EPR spectra of **DMPO** (0.03 M) upon reaction with 10 mM H_2O_2 and 1 mM FeSO_4 in H_2O . Microwave Freq. 9.44 GHz, power 1.8 mW; Mod. Amp. 0.2 mT, Freq. 100 KHz; $T = 293$ K.

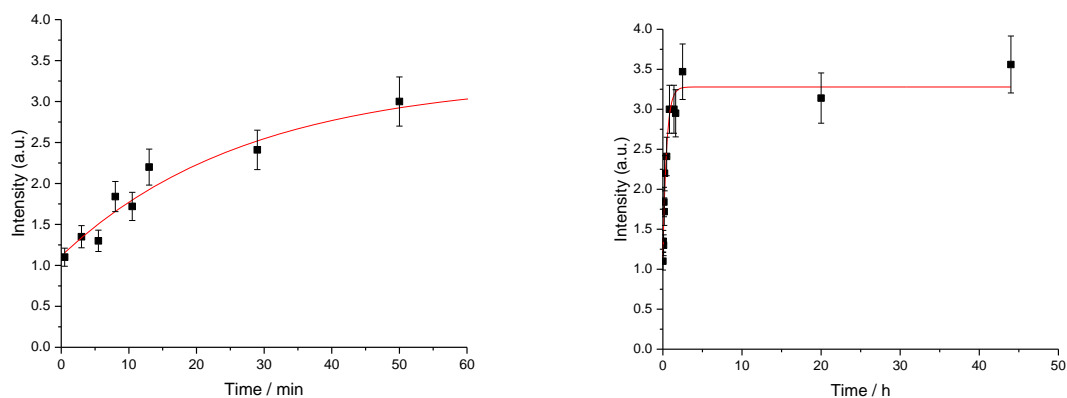


Fig S29. Evolution of the total integrated area of the EPR signal as a function of time for a 0.03 M solution of **5Eu** in the presence of 10 mM H_2O_2 and 1 mM FeSO_4 in H_2O at $T = 293$ K.

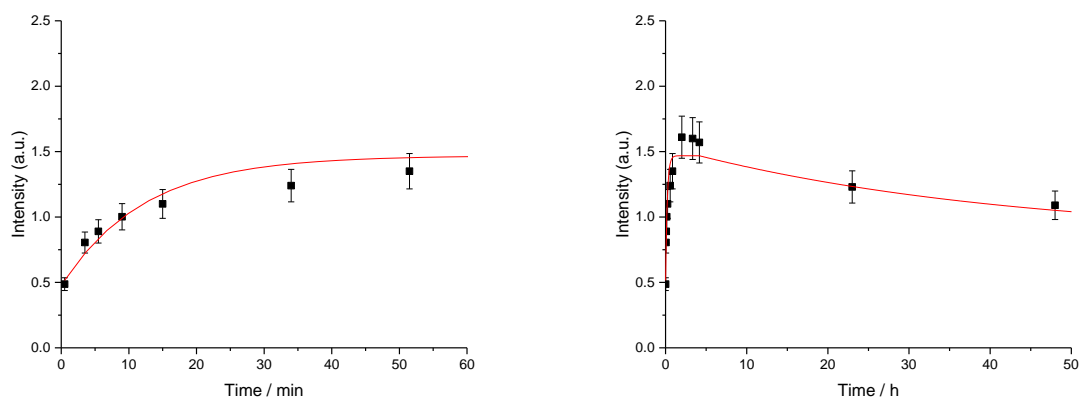


Fig S30. Evolution of the total integrated area of the EPR signal as a function of time for a 0.03 M solution of **5Yb** in the presence of 10 mM H_2O_2 and 1 mM FeSO_4 in H_2O at $T = 293$ K.

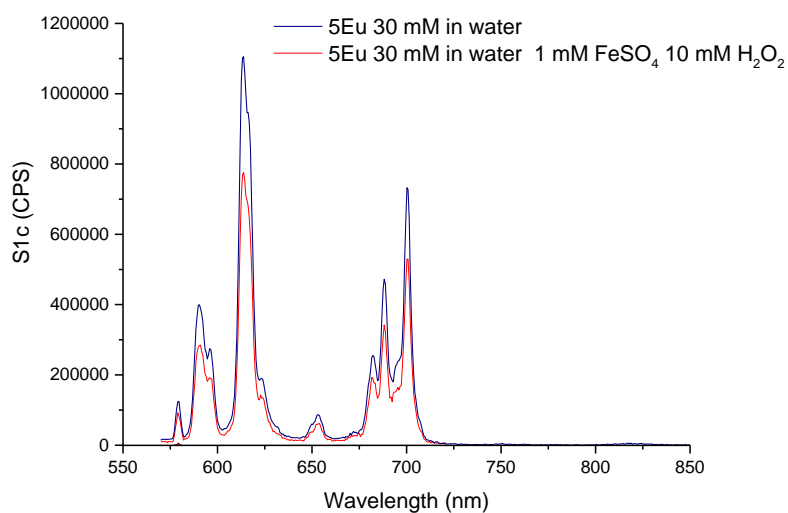


Fig S31. Raw emission spectra ($\lambda_{\text{ex}} = 325$ nm) of **5Eu** in 0.03 M aqueous solutions after 6 days. Black line = Blank; Red line = after 6 days in reaction with 10 mM H_2O_2 and 1 mM FeSO_4 . $T = 293$ K.

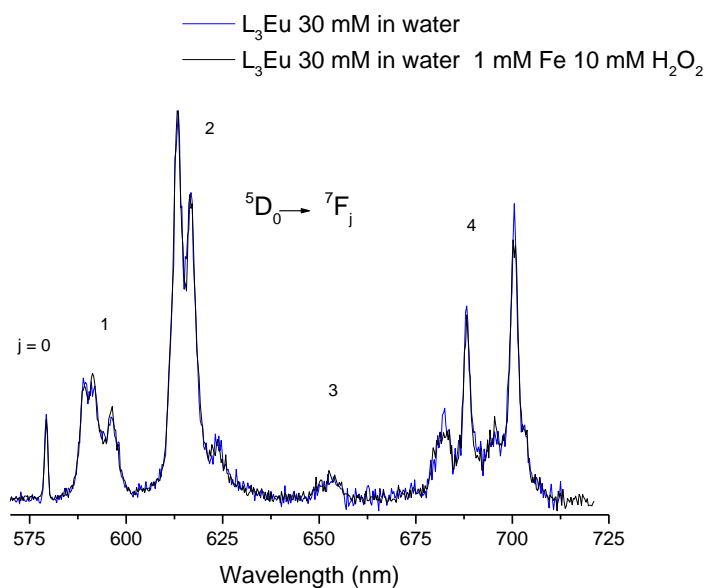


Fig S32. Normalized emission spectra ($\lambda_{ex} = 325$ nm) of **5Eu** in 0.03 M aqueous solutions after 6 days. Dark blue = Blank; Black line = after 6 days in reaction with 10 mM H_2O_2 and 1 mM $FeSO_4$. $T = 293$ K.

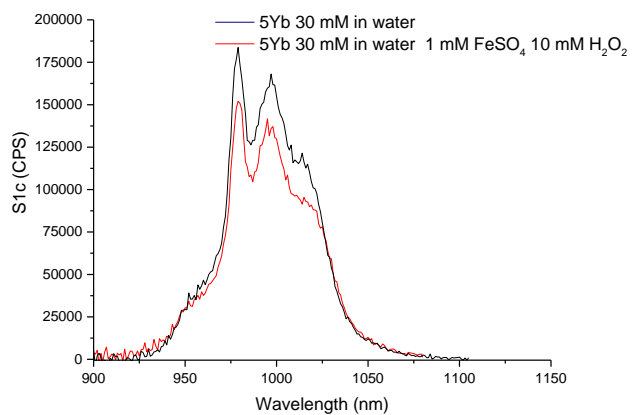


Fig S33. Raw emission spectra ($\lambda_{ex} = 325$ nm) of **5Yb** in 0.03 M aqueous solutions after 6 days. Dark blue = Blank; Red line = after 6 days in reaction with 10 mM H_2O_2 and 1 mM $FeSO_4$. $T = 293$ K.

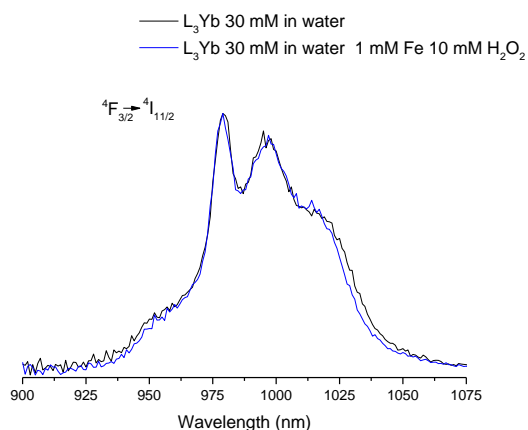


Fig S34. Normalized emission spectra ($\lambda_{\text{ex}} = 325 \text{ nm}$) of **5Yb** in 0.03 M aqueous solutions after 6 days. Dark blue = Blank; Black line = after 6 days in reaction with 10 mM H_2O_2 and 1 mM FeSO_4 . $T = 293 \text{ K}$.

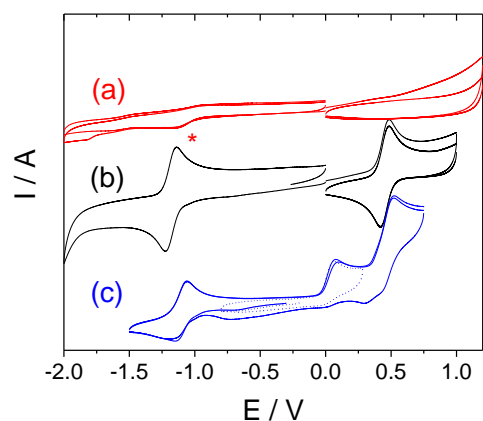


Fig S35. Cyclic voltammetry curves of (b) **3** and (c) **4** in 0.5 mM CH_3CN (+0.1 M TBAP) solution at a vitreous carbon electrode. (a) represents the CV curve of the solvent (the stars denotes the reduction wave of dioxygen). $T = 298 \text{ K}$. Reference = AgNO_3 0.01 M (remove ca. 0.09 V to convert vs. Fc^+/Fc).

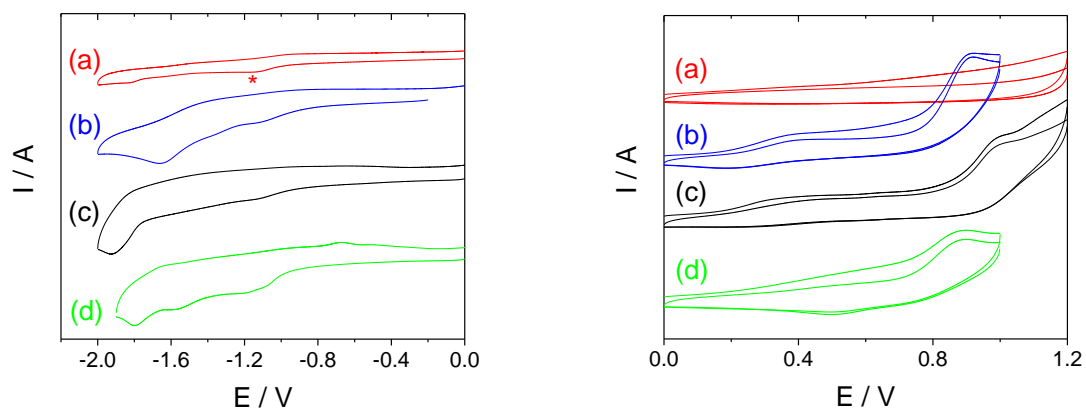


Fig S36. Cyclic voltammetry curves of (b) **5**, (c) **5Yb** and (d) **5Eu** 0.5 mM CH₃CN containing 2% water (+0.1 M TBAP) solution at a vitreous carbon electrode. (a) represents the CV curve of the solvent (the stars denotes the reduction wave of dioxygen). T = 298 K. Reference = AgNO₃ 0.01 M (remove ca. 0.09 V to convert vs. Fc⁺/Fc).

3. Tables

Table S1. Rate constants (in min^{-1}) for the formation (k_{growth}) and quenching (k_{decay}) of the radical species at 293 K. The radicals are generated from 0.03 M solutions of **5Yb** or **5Eu** in the presence of 10 mM H_2O_2 and 1 mM FeSO_4 in H_2O .

	k_{growth}	k_{decay}
DMPO	-	0.32(3)
Iminonitroxide / 5Eu ^[a]	0.15(2)	0.0019(3)
Nitronylnitroxide / 5Eu ^[b]	0.0048(7)	-
Total intensity / 5Eu	0.039(1)	-
Iminonitroxide / 5Yb ^[c]	n.d. ^[e]	0.0028(7)
Nitronylnitroxide / 5Yb ^[d]	0.010(2)	-
Total intensity / 5Yb	0.04(1)	n.d. ^[e]

^[a] Calculated from the relative intensity (in %) with respect to the maximum yield in iminonitroxide radical (set to 100 % at 50 min)

^[b] Calculated from the relative intensity (in %) with respect to the maximum yield in nitronylnitroxide radical (set to 100 % at 50 h)

^[a] Calculated from the relative intensity (in %) with respect to the maximum yield in iminonitroxide radical (set to 100 % at 5 min)

^[b] Calculated from the relative intensity (in %) with respect to the maximum yield in nitronylnitroxide radical (set to 100 % at 50 h)

^[e] Too fast (nitronylnitroxide) or too slow (total intensity) for an accurate determination.

Table S2. Electronic sub-levels of the $\text{Eu}(^7\text{F}_j)$ manifold ($J = 1-4$) in **5Eu** as determined from excitation and emission spectra at 295 K; $^5\text{D}_0$ is taken as the origin.

$^5\text{D}_0$	$^7\text{F}_1$	$^7\text{F}_2$	$^7\text{F}_3$	$^7\text{F}_4$
17265	293	909 sh	1880	2594
	350	957 max	1974	2734
	486	1047		2878
		1099 sh		2983
		1219		

4. References

1. G. Paolucci, A. Zanella, M. Bortoluzzi, S. Sostero, P. Longo and M. Napoli, *J. Mol. Catal. A: Chem.*, 2007, **272**, 258-264.
2. S. Stoll and A. Schweiger, *J. Magn. Res.*, 2006, **178**, 42-55.